

## Property Estimation for Pyrolysis Modeling Applied to Polyester FRP Composites with Different Glass Contents

by

Esther Kim<sup>1</sup>  
Chris Lautenberger<sup>2</sup>  
Nicholas Dembsey<sup>1</sup>

<sup>1</sup> Worcester Polytechnic Institute  
Department of Fire Protection Engineering  
100 Institute Road  
Worcester, MA 01609

<sup>2</sup> University of California, Berkeley  
Department of Mechanical Engineering  
Berkeley, CA 94720

### Abstract

For the composites industry to “design for fire” more thorough understanding of how typical FRPs decompose under fire conditions is needed. The role played by the glass and the resin (and additives) for FRPs are keys to understanding the fire behavior. To that end, this study continues work presented at Composites 2007 [1]. The goal of this work is to evaluate the ability of a pyrolysis model and genetic algorithm (optimization routine) pairing to estimate properties of each component of the composite, resin and glass. The composite pyrolysis experimental data used in this work was obtained from tests conducted on a bench scale fire test apparatus, Fire Propagation Apparatus, with additional instrumentation to measure surface and internal temperatures of the sample. Mass loss data and temperature profiles with respect to time at different in-depth locations are used in the optimization process. The property estimation exercise is conducted on a brominated, unsaturated polyester FRP composite with low glass content. Thermal analysis data from thermogravimetric analysis and differential scanning calorimetry of the polyester resin in the composite was used to model the decomposition kinetics. With the approximated decomposition kinetics for the resin, simulation of pyrolysis tests (nitrogen environment) of the composite slab was performed to estimate the unknown thermophysical properties by genetic algorithm optimization. A validation exercise

using the estimated properties is then conducted on a composite with high glass content. The quality of the estimated properties is assessed by comparing simulated results to experimental results for the high glass content sample.

### 1. Introduction

For the composites industry, designing for a FRP that provides good fire characteristics becomes a guess and check operation in many cases. Any changes made to the resin, glass, or the microstructure of the FRP affect the overall fire behavior of the FRP. Traditionally, the effect of the changes made in the FRP is checked by conducting tests via standard fire tests, which can be time consuming and expensive. Therefore, providing an understanding of how typical FRPs decompose under fire conditions and using this information to find an appropriate guideline for the composite industry to produce better fire-safe composites have been a long-term goal for this research. To that end, this work follows the work presented at Composites 2007.

In this study, complete data sets of decomposition of brominated, unsaturated polyester resin and its FRP composites with different glass contents are presented. Careful experiments were conducted using Thermogravimetric Analysis (TGA) and Differential Scanning Calorimetry (DSC) in order to study the thermal decomposition kinetics of the polyester resin. Also, the polyester FRPs with different glass contents – 33 wt% (1A) and 60 wt% (1C) – were tested under a modern bench-scale fire test apparatus known as Fire Propagation Apparatus (FPA, ASTM E 2058[2]) with additional instrumentations such as thermocouples at various depths. These tests were designed to generate data specifically useful for computer modeling purposes.

The model used in this study is a generalized pyrolysis model developed by Lautenberger [3,4], which simulates the heating and decomposition of a chosen material. Like with any other pyrolysis models, this model requires many input parameters found from material properties, which include the pyrolysis kinetics (pre-exponential factor, activation energy, reaction order), thermal properties (specific heat capacity, thermal conductivity), and radiative characteristics (surface emissivity, in-depth radiation absorption coefficient). Unfortunately, there are no standardized techniques to determine all of these properties via laboratory tests. Another way of estimating parameters is to use an optimization routine with a pyrolysis model in pair.

The current work applies Genetic Algorithm as an optimizing method coupled with Lautenberger’s pyrolysis model [3,4] to perform parameter estimation. Using the experimental data of the polyester FRP with lower

glass content (1A), an estimation exercise is conducted to find properties of the individual components of the composite, i.e., resin and glass, where one is decomposable while the other is inert, respectively. The estimated parameters for these components are used to model the pyrolysis of the same polyester FRP but with higher glass content (1C). The simulated 1C mass loss rate (MLR) and temperatures (TC) will be compared to those of actual experiments to evaluate the appropriateness of the estimation. Additionally, the estimated properties will be compared to those found from the literature [1,5] to check how consistent the estimations are.

## 2. Pyrolysis of FRP Composite

### 2.1. FRP composite description

The resin in this study is a commercially prepared unsaturated polyester resin with 20 wt% bromination for its fire retardancy built in to the carbon backbone. Antimony trioxide is added, which acts as a synergist that assists the flame retardancy of the polymer resin. Among the various effects of adding antimony trioxide, the major role of this additive is reacting with the halogen such as bromine and removing the radicals that are essential for combustion chemical reactions to proceed. This additive is also known to delay the escape of halogen from the flame, which increases its concentration and diluting effect [6]. The resin was catalyzed with methyl ethyl ketone peroxide (MEKP). According to the product description, this resin is a low viscosity, thixotropic polyester resin formulated to be Class I per ASTM E 84 [7] (flame spread index < 25 and smoke developed < 450).

Composite panels were fabricated by hand lay-up and vacuum bagging for low (33 wt% of glass, average thickness of 10 mm) and high (60 wt% of glass, average thickness of 6 ~7 mm) glass content composites, respectively, using two different types of fiberglass mats that were wetted with resin. The two types of fiberglass (E-glass) used in the composite are a chopped strand mat and a glass roving woven mat with an area density of 25 g/m<sup>2</sup> and 880 g/m<sup>2</sup>, respectively. The chopped strand mat is thinner and more porous than the woven mat. The laminate schedule (provided by the manufacturer) is chopped strand mat and roving alternating five times for 1A and eight times for 1C with another chopped strand mat layer at the end. Visual inspection of a polished cross-section of the composite slab is consistent with this laminate schedule, but with polymer resin layers between each fiberglass layer. The chopped strand mat layer is difficult to identify in the cross section, perhaps because more resin is soaked into this layer than the roving layer. The roving layer is observed as a prominent glass layer possibly because the resin is absorbed only at the fiberglass layer surfaces leaving the interior with primarily glass.

The layered microstructure is determined to a resolution of 0.10 mm and 0.06 ~ 0.07 mm for 1A and 1C, respectively by inspecting a polished cross-section of the composite under a microscope. Based on visual observation and comparison to global density of the composite sample, approximations of three distinct layers are proposed: 100% resin, 100% glass, and 50% resin/50% glass. The microstructure is shown schematically in Figure 1. The lightest “box” represents 100% resin, the medium darkness box represents 50% resin/50% glass, and the darkest box represents 100% glass. Each box has a thickness of 1% of each sample’s average thickness.

### 2.2. Thermogravimetric Analysis (TGA) and Differential Scanning Calorimetry (DSC)

The instruments used in this study were manufactured from PerkinElmer: Thermogravimetric Analysis 7 (TGA7) and the Differential Scanning Calorimetry 7 (DSC7). Throughout this study, TGA and DSC were used for a non-isothermal test purposes and the tests were conducted in a nitrogen environment. Using TGA7, 4 different heating rates of 5°C/min., 10°C/min., 30°C/min. and 50°C/min. were applied to measure the mass loss history of each resin sample. For each test, a sample amount of 7.5 mg ~ 10.5 mg was used. TGA7 was calibrated using 4 different standard reference materials over the temperature range of ambient to 850°C: Alumel, Nickel, Perkalloy and Iron. Each reference was checked for its magnetic transition temperatures, which should be within +/- 5°C of its reported values. For DSC7, constant heating rates of 10°C/min., 30°C/min., 50°C/min. and 70°C/min. were used to measure the heat flow through the sample during its thermal decomposition. A sample amount of 7.5 ~ 9.5 mg was used for each test. This instrument was calibrated using the standard indium and zinc references for a temperature range of ambient to the maximum temperature available from the instrument, 500°C. The melting points of these references were checked to be within +/- 10% of its reported values. The enthalpy check was performed using indium. The heat of fusion for indium was calibrated to be within 10% of its reference value. A simple baseline subtraction was conducted to eliminate the unnecessary curvatures within the heat flow curve.

### 2.3. Fire Propagation Apparatus (FPA)

Similar to the Cone Calorimeter (Cone, ASTM E 1354[8]), the Fire Propagation Apparatus (FPA, ASTM E 2058[9]) is a bench-scale fire test apparatus in which the sample is heated by four radiant lamps as opposed to using an electrically heated coil as a radiant source as in the Cone. There are 6 bulbs within one IR lamp that consist a tungsten wire in argon gas. These bulbs emit with a narrow energy spectrum where the peaks are 1.15 and 0.89 microns [10]. Based on experimental analysis, the lamps are known to provide a uniform heat flux that

is steady within  $5\text{kW/m}^2$  over the specimen surface of up to  $60\text{kW/m}^2$ . A long quartz tube is used to create a desired atmosphere. The atmosphere may be controlled from nitrogen to 40% enhanced oxygen condition. A flow rate of 100 or 200 lpm is run through the bottom of the air chamber depending on the purging gas and therefore the sample is in a flow field during the test. The FPA can be used to calculate useful engineering data such as carbon dioxide generation based heat release rate (based on the standard), mass loss rate, smoke yield and smoke extinction coefficient.

The purpose of FPA testing was to generate good data sets appropriate for pyrolysis modelling and parameter estimation, and therefore several modifications were made to the standard testing procedure. First, when testing the polyester FRPs, an insulated sample dish purposed by de Ris and Khan [11] was used instead of the standard specified, non-insulated aluminium dish (see Figure 2). In this sample dish, the sample is surrounded by Cotronics® paper insulation on the back and sides to limit heat loss, which simplifies the pyrolysis modeling. Second, 4 thermocouples were installed to measure temperature change of the sample at various depths: surface, 1/3, 2/3 and back face of the sample. The installation of thermocouples on the sample was consistent with the method introduced in Composites 2007 paper [1]. Based on experimental analysis, a zone of uniformity with regards to temperature and heat flux was found to be within 32 mm (1.25 in.) radius from the center of the specimen and therefore, all four thermocouple beads were located within this zone. Thermocouple holes were drilled at 1/3 and 2/3 of the sample thickness with a 1.25 mm diameter drill bits. Thermal grease (OmegaTherm Thermally Conductive Silicone Paste, Model OT-201 from Omega Engineering) was inserted along with the thermocouples (Omega Precision Fine Wire Thermocouples, Model 5TC-GG-K-30-36 from Omega Engineering) to reduce the air gaps within the thermocouple holes. The surface and back face thermocouples were affixed with a high temperature adhesive (Resbond 907 Industrial Strength Fireproof Adhesive from Cotronics Corp.) and Crazy glue, respectively. Third, carbon black was applied on the sample surface to allow radiation to be absorbed on the surface of the sample. This approach was taken because the samples (1A and 1C) were somewhat transparent and when tested in the FPA, in-depth absorption of radiation occurred. To incorporate in-depth absorption of radiation into the model requires more parameters than assuming only surface absorption. Therefore, to minimize the number of parameters that need to be optimized, carbon black was used which, should allow surface radiation absorption only. All of the tests were conducted under nitrogen to eliminate the effect of oxidation in the resin degradation kinetics and flame. Limiting the environment to only nitrogen allowed for more simplified kinetics modeling for the resin degradation as well as the pyrolysis modeling of the composite.

The uncertainty for the mass loss rate (MLR) and thermocouple measurements were determined via statistical analysis performed on data from tests with identical conditions. All uncertainties listed in this study are full scale (as opposed to  $\pm$  half scale). The uncertainty of MLR for the FPA was determined as  $17\text{mg/s}$  ( $2.4\text{g/sm}^2$ ) by comparing three PMMA tests performed at  $50\text{kW/m}^2$  based on the standard which calls for three identical tests to be performed to correctly determine other properties [10]. The uncertainty in the thermocouple measurements was quantified by comparing back face temperature data from four identical 1C tests in the FPA. Temperature measurement at the back face of the sample surface was chosen because the exact measurement location is known, i.e. the sample thickness. Other temperature measurements made in various depths have a positional uncertainty of  $\pm 0.625$  mm associated with the data. This uncertainty is from the drill bit used to make holes for thermocouple installations, which had a thickness of 1.25mm diameter. Using the normalized time, time divided by sample thickness square, i.e.,  $\tau = \text{time}/\delta^2$  to remove the effect of different sample thicknesses when comparing, the maximum deviation at various normalized times, up to the critical time,  $\tau_c$ , was  $16^\circ\text{C}$ . The critical time,  $\tau_c$ , corresponds to the time when evenly spread flame on sample surface disappearing when tested under air. Test data presented in this parameter estimation exercise study is truncated at this critical time of 4 s/mm<sup>2</sup> because the pyrolysis model is set up with a one-dimensional assumption, which may not be used when flames on the sample surface is not evenly distributed, typically where edge burning is dominant. These uncertainty values will be used to evaluate significant differences in the modeling results

### 3. Pyrolysis Modeling for Lumped (TGA) and Slab (Cone or FPA) Experiments

The calculations reported here are conducted with a generalized pyrolysis model [3,4] that can be applied to a wide variety of condensed phase fuels. The model simultaneously calculates the condensed phase mass conservation, gas phase mass conservation, condensed phase species conservation, and condensed phase energy conservation equations. This model can be applied to both 0D and 1D systems and is therefore capable simulating both “lumped” (thermogravimetric) and “slab” (Cone Calorimeter/FPA) experiments. Extensive details are given in Ref. [3,4] so only a brief overview is given here. Assumptions inherent in the model, as applied in this paper, include:

- Porosity can either be solved as a property of a species (default) or directly. When porosity is solved directly, it is derived from the condensed-phase mass conservation equation assuming no volume change (shrinkage or swelling).

- When porosity is directly solved, the user-specified thermal conductivity and density are interpreted as those of a nonporous solid. Therefore, the thermal conductivity that appears in the condensed-phase energy conservation equation is  $\bar{k} = (1-\psi)\bar{k}_s$  where  $\psi$  is porosity and  $\bar{k}_s$  is the weighted thermal conductivity of the solid assuming it is nonporous. Similarly, with this formulation, the bulk density is calculated as  $\bar{\rho} = (1-\psi)\bar{\rho}_s$  where  $\bar{\rho}_s$  is the weighted density of the solid assuming it is nonporous.

- Bulk thermal conductivity  $\bar{k}$  has a cut-off value of 0.03W/mK which corresponds to air at 300 to 400K.

- Specific heat is calculated with a weighted or averaged quantity, i.e.  $\bar{c}_p = \sum X_i c_{p_i}$  as other solid properties – enthalpy, emissivity, radiation absorption coefficient, permeability, etc.

- Specific heat capacity and effective thermal conductivity vary by as  $k(T) = k_0(T/T_r)^{n_k}$  and  $c(T) = c_0(T/T_r)^{n_c}$ , respectively, where  $T_r$  is a reference temperature.

- Radiation heat transfer across pores is accounted for by adding a contribution to the effective thermal conductivity that varies as  $\gamma T^3$ , where  $\gamma$  is a fitting parameter

- Averaged properties in conservation equations are calculated by appropriate mass or volume fraction weighting

- All gases escape to the exterior ambient with no resistance to heat or mass transfer

- Negligible heat transfer between the gas phase and the condensed phase inside the decomposing solid

- There is no net shrinkage (volume change) due to reactions or bulk density changes

- 

## 4. Results and Discussion

### 4.1. Kinetics of resin degradation

Typically in kinetic studies, the isothermal rate of degradation or conversion,  $d\alpha/dt$ , is assumed to be a linear function of the temperature dependent rate constant,  $k(T)$ , and a temperature independent function of the conversion,  $f(\alpha)$ , where  $\alpha$  indicates the conversion. This equation can be further expanded by using the Arrhenius

expression for the rate constant. Within the Arrhenius expression, two more reaction dependent constants are introduced: the pre-exponential constant,  $Z$ , and the activation energy,  $E_a$ . The temperature independent function of the conversion,  $f(\alpha)$  is dependent upon the mechanism of chemical reactions.

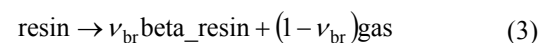
$$\frac{d\alpha}{dt} = f(\alpha)Z \exp\left(-\frac{E_a}{RT}\right) \quad (1)$$

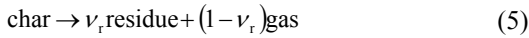
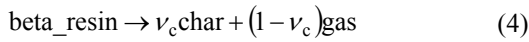
Substituting the linear heating rate  $\beta = dT/dt$  into Eq. (1) and taking the natural logarithm of both sides gives the following:

$$\begin{aligned} \ln \frac{d\alpha}{dT} &= \ln \left( \frac{f(\alpha)}{\beta} Z \exp\left(-\frac{E_a}{RT}\right) \right) \\ &= \ln \left( \frac{f(\alpha)Z}{\beta} \right) - \frac{E_a}{RT} \end{aligned} \quad (2)$$

The iso-conversional method, also known as the model-free method is used to find the minimum number of elementary reactions necessary to describe the global degradation kinetics of the resin. This method uses data tested from different heating rates. Knowing that at a constant conversion,  $\alpha$ ,  $d\alpha/dt$  and  $f(\alpha)$  become constants. With these terms in Eq.(2) remaining as constants, the  $E_a$  is found without the pre-knowledge of the reaction mechanisms. The iso-conversional method will give constant activation energies,  $E_a$ , over the range of conversion of interest if the reaction is a single-step chemical reaction. If the activation energies,  $E_a$ , changes significantly with respect to different conversions, this is an indication for a more complex reaction mechanism.

In Figure 3, the results from two iso-conversional methods introduced by Ozawa, Flynn and Wall [12,13] (OFW, finding a constant slope of  $-E_a/R$  by plotting  $\ln(\beta)$  versus  $1/T$ ) and Friedman [ 14 , 15 ] (plotting  $\ln(da/dT)$  versus  $1/T$  to find the slope of  $-E_a/R$ ) conducted on the polyester resin are shown. Both methods are used for comparison purposes. The r-square values for each activation energy value are plotted as well using least square method. The activation energy becomes more reliable as the r-square values become closer to 1. The conversion is calculated as  $\alpha = 1 - m/m_0$ . As shown in Figure 3, the estimated activation energy ranges from 70 ~ 145 kJ/mol in  $0 < \alpha < 0.20$ , relatively steady around 120 ~ 145 kJ/mol in  $0.20 < \alpha < 0.93$  and 145 kJ/mol and above in  $0.93 < \alpha < 1.0$ . Based on this result, one can approximate a minimum of three elementary reactions to model the full degradation over  $0 < \alpha < 0.97$  range.





The proposed mechanism is consistent with previous research [16,17,18] conducted for unsaturated polyester thermoset resins. In addition to this three steps mechanism, a single step degradation mechanism of resin becoming char and releasing fuel gas (93% weight loss) is modeled and compared to evaluate the necessity of multiple reaction steps. Applying these degradation mechanisms, a model fitting method [19] is used where  $f(\alpha)$  is preselected to fit the TGA experiment data to find the kinetic parameters with the best fitness. In this study, a conversion function  $f(\alpha) = (1 - \alpha)^n$  is used, which is typically applied for phase boundary reactions. The data fitting software used in this study is Genetic Algorithm (GA) coupled with the pyrolysis model for lumped experiments explained in the previous section. The GA was developed based on the mechanics of the Darwinian survival-of-the-fittest theory [3,4,20].

The results found from model fitting exercise are summarized in Table 1 and plotted in Figure 4. As shown in Figure 4, using three steps when modeling the resin degradation gives better fitness of the estimated mass loss rate to the actual TGA experiment data. When three steps are used instead of one, the initial mass loss that starts from 200°C is captured while the temperature needs to increase up to 300°C to initiate any mass loss when using one step reaction (see total mass loss rate in (a) and (c) of Figure 4). In addition to the earlier stage of degradation, better fitness is shown after 400 °C for the three steps reactions case than that of one step where mass loss rate is expected to rapidly decrease. The total mass loss rate peak observed in ~400°C range spreads over a wider temperature range when a single step reaction is used for resin degradation. This is due to the unresolved initial mass loss when using single step reaction. An additional mass loss is given at the end of the major mass loss peak after 400°C to compensate for the initial mass loss which should have existed before 200°C. However, these differences in mass loss rate found from applying two resin decomposition mechanisms – three steps vs. single – are subtle. Comparing the difference at various heating rates emphasizes more that the effect of changing resin degradation mechanism from 3 steps to single is insignificant (see (b) and (d) of Figure 4).

#### 4.2. Property estimation for FRP composite using polyester composite with low glass content (1A)

The property estimation for the polyester composite is conducted by coupling a generalized pyrolysis model for slab experiments developed by Lautenberger and the

Genetic Algorithms (GA) for optimization routine [3,4,20]. To reduce the number of parameters to estimate, the FPA experiments for the polyester composite with low glass content, 1A were conducted with certain approaches. For example, carbon black powder was applied on top of the sample surface to eliminate in-depth absorption of radiation. FPA tests were conducted under nitrogen environment to exclude the effect of oxidative decomposition of the resin and flame. Experimental data used in the estimation exercise was truncated when normalized time, time divided by sample thickness square, i.e.,  $\tau = \text{time}/\delta^2$  became approximately 4 s/mm<sup>2</sup>. This time is noted as the critical time,  $\tau_c$ , for a typical 1A sample when the pyrolysis can no longer be simplified as a one-dimensional problem. The critical time,  $\tau_c$ , is identified as time of evenly spread flame on sample surface disappearing when tested under air, where edge burning is dominant. Additionally, for further simplification of the problem when modeling, the backface temperature measurement was used as a boundary condition for the condensed phase.

The parameter estimation exercise was conducted for the following two cases: (1) GA1 where the heterogeneous microstructure was incorporated and three steps mechanism for resin decomposition was used; (2) GA2 where a single layer was constructed as a homogeneous structure based on resin and glass weight proportion within the composite and three steps mechanism for resin decomposition was used. For both cases, the same set of parameters is optimized, which are listed in Table 2 along with the estimation results. These parameters were introduced in Section 3 where a brief description of the pyrolysis model used in this study [3,4] is given. The kinetic parameters for resin degradation were predetermined as described in the previous section. However, the heats of reaction for the three elementary reactions were estimated through parameter estimation exercise as other thermophysical properties, but with its searchable range for optimization set based on Differential Scanning Calorimeter (DSC) experiment results on the polyester resin. Note that the heat of reactions were proportioned to reflect the kinetic modeling, i.e. the first, second and third reactions consumes 20%, 73% and 8% of the total enthalpy, respectively, which is identical to the resin weight loss percentages in each reaction step. The total number of parameters that was found via optimization was 29 including the heat of reactions. These estimations are used as two different baselines – GA1 and GA2 – for pyrolysis modeling study discussed in the next section. In Table 2, the estimation of GA1 and GA2 are compared to show how consistent the estimations are. It shows that most of the estimated values of GA2 have a difference of less than 30% when compared to those of GA1, which allows constructing some level of confidence in the optimizing capability of the Genetic Algorithms. Although the comparison has been made for individual parameter estimations and shown that results

from GA1 and GA2 are somewhat consistent, one should take into account that the Genetic Algorithm optimizes for a group of these individual estimations that gives the best fit to the mass loss rate and temperature data measured at four locations. When compared in groups, typically it shows that a change occurred in one parameter is compensated by a change found from the other. Hence, comparing the pyrolysis modeling results using the estimations from two different set-ups (GA1 and GA2) in groups should present a better sense of optimization consistency.

Using the estimated properties found from GA1 and GA2 conditions, four cases (as summarized in Table 3) for 1A (sample with low glass content) are modeled to check the fitness of the optimization and compare cases with various modeling conditions (see Figure 5 and Figure 6). These cases are constructed based on applying different assumptions for the microstructure of the composite (heterogeneous or homogeneous) and degradation mechanism (3 steps or single). For every case, the pyrolysis modeling results of mass loss rate and temperatures from surface, 1/3, 2/3 of sample thickness from surface, and backface are plotted with the actual experimental data. The parameter estimations from GA1 and GA2 set-ups should give the best fit for case 1 and case 2, respectively because the optimization was performed based on the corresponding conditions.

In general, from Figure 5 and Figure 6 one can conclude that the parameter estimations for 1A with two set-ups – GA1 and GA2 – were conducted properly and that the two baselines are nominally equivalent knowing that both modeling results are in a good agreement with the actual experiment data within the uncertainty stated for the experiment (17mg/s and 16°C for mass loss rate and temperature measurements, respectively). This also demonstrates that the parameter estimations for GA1 and GA2 conditions are consistent. In both figures, (a) shows that modeling the mass loss rate had improved qualitatively when microstructure of composite was incorporated as an input (case1 and case3) as oppose to simply assuming as a homogeneous material (case 2 and case 4). However, note that quantitatively the changes should be considered as insignificant taking into account for the uncertainty of 17mg/s. The mass loss rate data shown in the figures were applied with Fast Fourier Transform (FFT) smoothing, which resulted in artificial oscillations with magnitude in the order of 0.01g/s. Therefore, the actual mass loss rate has an initial peak before  $\tau = 1$ , another smaller peak following around  $\tau = 1.4$  with a decreasing trend up until  $\tau = 1.8$ , and a slowly increasing trend from that point to  $\tau = 4$ . The minimal point in the mass loss rate data near  $\tau = 1.8$  is possibly due to pyrolysis proceeding through the prominent glass layer after decomposing through the resin rich layers. The model was able to capture the large oscillations in the beginning and the decreasing trend followed by an increasing trend

near  $\tau = 1.8$  in the mass loss rate generated by pyrolyzing through different layers composed of an alternating decomposable resin and inert glass layers. The simulated temperature results follow well with the actual tests data for all four cases. Note that even with this comparison made without incorporating the positional uncertainty of  $\pm 0.625$  mm for the in-depth thermocouple installation to the temperature measurement uncertainty band, the simulation and actual test data show a good agreement (see (c) and (d) in Figure 5 and Figure 6). The simulation and actual data for backface temperature is shown in (e) in Figure 5 and Figure 6 as a check to confirm they match perfectly knowing that this was used as a boundary condition in the simulation. Changing the resin decomposition mechanism from 3 steps to a single step had an insignificant effect on the simulation results, which is consistent with the results found from kinetic modeling analyses performed in the previous section.

Based on the findings from above analyses, one can conclude the following: (1) Optimization for parameter estimation using pyrolysis model with GA was conducted with satisfaction in terms of mass loss rate and temperatures at various depths (surface, 1/3 and 2/3 in-depth from surface, and backface) for both conditions with consistency – GA1 and GA2. Quantitatively, the two baselines are nominally equivalent considering the uncertainty associated with the experimental data. (2) Incorporating the microstructure of the composite improves the mass loss rate simulations in terms of resolving the detailed oscillations and following the trend qualitatively but has less impact on sample temperature predictions. (3) Applying 3 steps resin decomposition mechanism than a single step has subtle influence in the modeling results.

### 4.3. Evaluation for estimated properties

To evaluate the correctness of the property estimation, modeling of the same composite as 1A but with higher glass content designated as 1C is conducted. The parameter estimation using 1A pyrolysis FPA test data was for the resin and glass. In theory if the parameter estimation was conducted properly, one should be able to model a composite that is produced with the same type of resin and glass using the estimation as an input to the pyrolysis model with the degrees of satisfaction which was found from comparing the modeling results for 1A as shown in Figure 5 and Figure 6.

Four cases as in Table 3 for 1C with two baselines – GA1 and GA2 – are simulated using the estimated properties found from 1A. The results are shown in Figure 7 and Figure 8 where mass loss rate and temperature measurements from surface, 1/3 and 2/3 of sample thickness from surface, and backface are plotted with experimental data. As it was with 1A simulations, applying

GA1 or GA2 as a baseline have an insignificant effect on the 1C modeling results. In both Figure 7 and Figure 8, (a) shows that the simulation results of case 2 and 4 (homogeneous structure with 3 steps or single step resin decomposition mechanism assumptions) have the better fit to the actual test data considering the uncertainty of 17mg/s than those of case 1 and 3 (heterogeneous structure with 3 steps or single step resin decomposition mechanism assumptions). Although incorporating the microstructure of the composite (assuming heterogeneous) does allow the model to resolve the oscillations in the mass loss rate curve due to pyrolysis through resin and glass alternating layers (case 1 and case 3), this phenomenon is not observed from the experiment. The difference of modeled temperatures at various depths and those from the actual experiment are within the measurement uncertainty and the positional uncertainty of  $\pm 0.625$  mm for the 1/3 and 2/3 in-depth thermocouple bead where temperature is actually measured (see (b) through (d) in Figure 7 and Figure 8). The positional uncertainty associated with the 1/3 and 2/3 in-depth thermocouple location is interpreted in the context of the simulation results. This is conducted by comparing the simulated temperatures from the exact 1/3 and 2/3 locations as well as temperatures at  $\pm 0.625$  mm from the exact locations. The simulation and actual data for back-face temperature is shown in (e) in Figure 7 and Figure 8 as a check to confirm they are identical knowing that this was used as a boundary condition in the simulation. Similar to 1A simulation results, using either 3 steps or a single step for the polyester resin decomposition mechanism was irrelevant in terms of simulating mass loss or temperature changes of 1C.

Comparing the results from pyrolysis modeling of 1C (see Figure 7 and Figure 8) to those of 1A (see Figure 5 and Figure 6), one can find that the major difference is observed from the mass loss rate simulations. In 1C simulations, for both GA1 and GA2 conditions, incorporating the microstructure of the composite have a negative effect on the mass loss rate simulation while it has a positive effect qualitatively when simulating 1A. To find a plausible explanation for this difference, additional pyrolysis modeling numerical experiments were conducted for 1C. For these numerical experiments, minor adjustments to the 1C microstructure were made for the following reason. More uncertainty is introduced when 1C microstructure is estimated visually than for 1A because in 1C (average thickness of 6 ~ 7 mm) more layers are added to a thinner sample comparing to 1A (average thickness of 10 mm). As shown in (a) of Figure 7 and Figure 8, the simulation with heterogeneous structure allows an over-prediction of the mass loss rate between  $\tau = 1$  and 2 and under-prediction between  $\tau = 2$  and 3. This indicated that the proposed microstructure (see Figure 1) for 1C used in the model had more resin on surface than actual followed by layers with more glass than actual. Therefore, when running the model, slight mod-

ification was made to the 1C microstructure near the surface within 0.5 mm to resolve the identified problem but the global density was maintained to 40 wt% resin and 60 wt% glass. The simulation results are shown in Figure 9. As shown in this figure, using the same estimated parameters the mass loss rate simulation can be improved without negatively affecting the temperature agreement by simply adjusting the microstructure only to a minimal degree. Therefore, it shows that the simulation agreement with the actual data is sensitive to the microstructure as oppose to the parameter estimation was poorly conducted.

To check whether the estimated parameter values from this study are consistent with other references [1,5], a comparison is made for the conductivities and the specific heat capacities of the virgin composite (resin and glass), decomposed composite (char and glass) and fully decomposed composite (glass only). An artificial composite is made with 30 wt% of resin and 70 wt% of glass with the estimated parameters from 1A FPA pyrolysis tests to directly compare the values found from Lattimer's paper [5] where conductivities and heat capacities are experimentally evaluated for a glass reinforced vinyl ester composite found from different stages of pyrolysis. The method used to determine the thermal properties found from Lattimer's work incorporates the effects of voids and cracks generated during pyrolysis. Therefore, effective thermal conductivity and heat capacity are used to compare with Lattimer's data, which are calculated based on volume fraction including the properties of the voids as gas. In addition to Lattimer's data, thermal properties estimated for 1A and 1Cs by Avila [1] are plotted for more comparison. As shown in Figure 10, the effective thermal properties calculated from estimated parameters using 1A test data for both GA1 and GA2 conditions are consistent with other reference values. The average deviation of the estimations found from this study is within 50% of those of Lattimer and Avila for conductivity and heat capacity.

## 5. Conclusions and Future Work

A property estimation exercise for pyrolysis modeling is conducted on unsaturated polyester FRP composites with low glass content (1A). To properly model the pyrolysis of the composite, kinetic modeling of the resin degradation was performed using TGA and DSC experiment data on the resin. Using an iso-conversional method (also known as model-free method), the minimum number of elementary reactions required to describe the full degradation mechanism was proposed. Based on this analysis, three steps mechanism was constructed. In addition to this three steps mechanism, a single step case was also investigated to compare the effect of using a more complicated approach than a simple one step on the overall pyrolysis modeling and property estimation. With

a pre-known reaction mechanism, a model fitting method was used to find the kinetic parameters for each reaction.

Property estimation for unsaturated polyester FRP composite was conducted using the 1A FPA pyrolysis test data with a generalized pyrolysis model, Gpyro paired with an optimization routine known as Genetic Algorithm (GA). Two conditions were used to construct a baseline – (1) GA1 where the heterogeneous microstructure was incorporated and three steps mechanism for resin decomposition was used; (2) GA2 where a single layer was constructed as a homogeneous structure based on resin and glass weight proportion within the composite and three steps mechanism for resin decomposition was used. Independent of applying one of these conditions, the estimation was conducted for the same set of parameters for resin and glass as summarized in Table 2.

The estimated values were used to model 1A to verify the fitness of the optimization and compare cases with different microstructures (heterogeneous or homogeneous) and kinetic mechanisms (3 steps or single step), which are designated as case 1 through 4. For both GA1 and GA2 conditions, the parameter optimization results showed that the pyrolysis modeling was conducted with satisfaction in terms of mass loss rate and temperatures at various depths (surface, 1/3 and 2/3 in-depth from surface, and backface). It also demonstrated that whether applying GA1 or GA2 conditions as a baseline, the simulation results are nominally identical quantitatively considering the uncertainty of the experiment data, however, estimation based on GA1 and GA2 conditions are consistent. The pyrolysis modeling results qualitatively showed that incorporating microstructure of the composite when modeling allows the model to resolve oscillations in the mass loss rate. Changing the kinetics mechanism had a subtle influence for modeling this composite.

To evaluate whether the estimation can represent the components of the composite, resin and glass, a pyrolysis modeling is conducted for a polyester FRP composite with higher glass content (1C) than 1A. The results show a relatively good agreement to the actual test data except for the mass loss rate. Although for 1A applying the heterogeneous microstructure to the modeling did improve the simulation results, it did not for 1C modeling. A reasonable explanation for this poor estimation is due to the uncertainty in the microstructure of 1C near the surface rather than poorly conducted parameter estimation. In addition to 1C modeling, estimated conductivity and heat capacity values are compared with those of other references and confirmed that it was consistent within 50%.

In this study, the work demonstrates the possibility of constructing a virtual experiment for composites using a bench-scale pyrolysis test and thermal analysis experi-

ment data. Using one type of composite (1A), an optimization of parameters was conducted and those estimations were used to model a different type of composite (1C). In the future, the work will be expanded to cases where fire retardant additives have an effect to the degradation kinetics of the composite and composites are decomposing in an oxidative condition such as air. The goal of the work will be to develop an approach that is consistent and simple when performing parameter estimation and modeling for different types of composites in various conditions.

## Acknowledgments

The authors would like to thank Charles Dore for fabricating and donating the polyester FRP composite materials used in this study. Many thanks also to Randall Harris, William Wong and Haejun Park at WPI for assisting the FPA tests.

## Reference

- <sup>1</sup> Avila, Melissa B., Dembsey, Nicholas A., Kim, Mi-hyun E., Lautenberger, Chris, Dore, Charles, Fire Characteristics of Polyester FRP Composites with Different Glass Contents, *Composites & Polymers 2007*, American Composites Manufacturers Association, October 17-19, 2007
- <sup>2</sup> Standard Methods of Test for Measurement of Synthetic Polymer Material Flammability Using a Fire Propagation Apparatus (FPA), ASTM E 2058-03, ASTM, 100 Barr Harbor Drive, West Conshohocken, PA, U.S.
- <sup>3</sup> Lautenberger, C., "A Generalized Pyrolysis Model for Combustible Solids", Ph.D. Dissertation, Department of Mechanical Engineering, University of California, Berkeley, Fall 2007
- <sup>4</sup> Lautenberger, C., Gpyro – A Generalized Pyrolysis Model for Combustible Solids Users' Guide, Version 0.609, July 23, 2008
- <sup>5</sup> Lattimer, Brian Y., Ouellette, Jason, Properties of composite materials for thermal analysis involving fires, *Composites: Part A 37* (2006) 1068–1081
- <sup>6</sup> Lewin, M., "Synergism and Catalysis in Flame Retardancy of Polymers", *Polym. Adv. Technol.* 12, 215-222 (2001)
- <sup>7</sup> Standard Test Method for Surface Burning Characteristics of Building Materials, ASTM E 84-05, ASTM, 100 Barr Harbor Drive, West Conshohocken, PA, U.S.
- <sup>8</sup> Standard Test Method for Heat and Visible Smoke Release Rates for Materials and Products Using an Oxygen Consumption Calorimeter, ASTM E 1354-02, ASTM, 100 Barr Harbor Drive, West Conshohocken, PA, U.S.
- <sup>9</sup> Standard Methods of Test for Measurement of Synthetic Polymer Material Flammability Using a Fire Propaga-



---

tion Apparatus (FPA), ASTM E 2058-03, ASTM, 100 Barr Harbor Drive, West Conshohocken, PA, U.S.

<sup>10</sup> User's Guide for the Fire Propagation Apparatus (FPA) ASTM E-2058, Fire Testing Technology Limited, PO Box 116, East Grinstead, West Sussex, England.

<sup>11</sup> de Ris, J.L. and Khan, M.M., "A sample holder for determining material properties," *Fire and Materials*, 24, 219-226 (2000).

<sup>12</sup> Ozawa, T., *Bull Chem Soc Jpn* 1965;38;188

<sup>13</sup> Flynn, J., Wall, L.A., *J Polym Lett* 1966;4:232

<sup>14</sup> Friedmen, H.L., *J Polym Sci Part C* 1964;6:183

<sup>15</sup> Friedmen, H.L., *J Polym Lett* 1966;4:232

<sup>16</sup> Chrissafis, K., Paraskevopoulos, K.M., Bikiaris, D.N., Thermal degradation kinetics of the biodegradable aliphatic polyester, poly(propylene succinate), *Polymer Degradation and Stability* 91 (2006) 60-68

---

<sup>17</sup> Y. S. Yang and L. James Lee, Microstructure formation in the cure of unsaturated polyester resins *Polymer*, Volume 29, Issue 10, October 1988, Pages 1793-1800

<sup>18</sup> Chiu, H.T., Chiu, S.H., Jeng, R.E., Chung, J.S., A study of the combustion and fire-retardance behaviour of unsaturated polyester/phenolic resin blends, *Polymer Degradation and Stability* 70 (2000) 505-514

<sup>19</sup> Burnham, A.K., Weese, R.K., Kinetics of thermal degradation of explosive binders Viton A, Estane, and Kel-F, *Thermochimica Acta* 426 (2005) 85-92

<sup>20</sup> Rein, G., Lautenberger, C., Fernandez-Pello, C., Toro, J.L., Urban, D.L., Application of genetic algorithms and thermogravimetry to determine the kinetics of polyurethane foam in smoldering combustion, *Combustion and Flame* 146 (2006) 95-108

Figures:

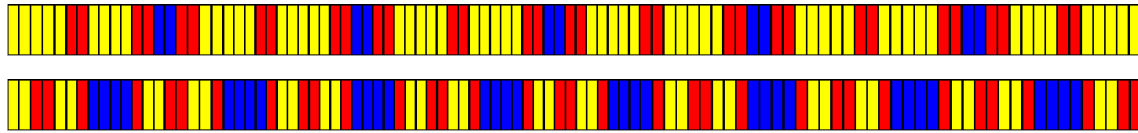


Figure 1: Approximation of three distinct layers – 100 wt% resin (yellow), 50-50 wt% resin and glass (red), and 100 wt% glass – in composite microstructure: Unsaturated polyester FRP with low glass content (1A, 33 wt% of glass, top) and with high glass content (1C, 60 wt% of glass, bottom)

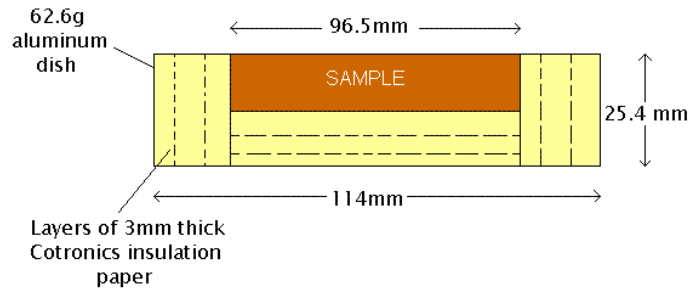


Figure 2: Insulated Sample Holder Designed by de Ris and Khan [11]

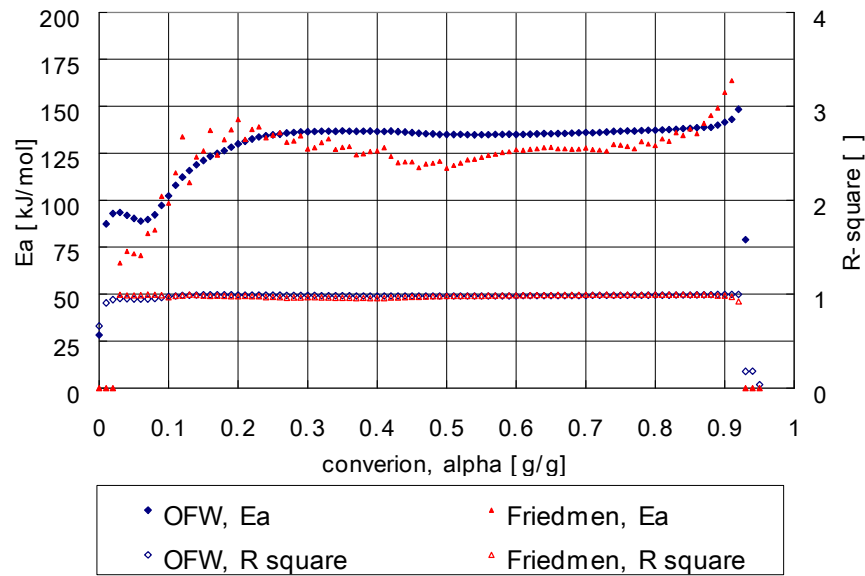
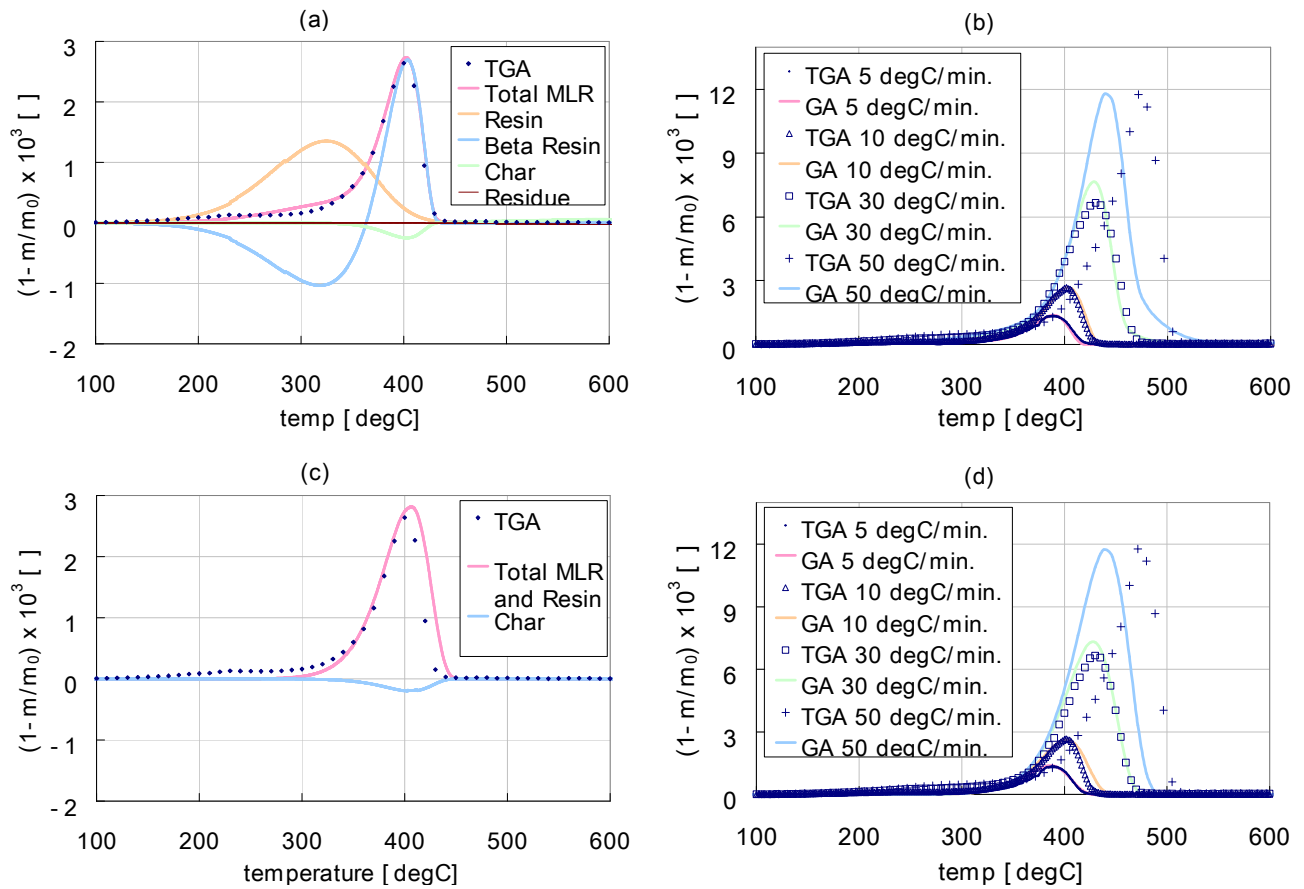
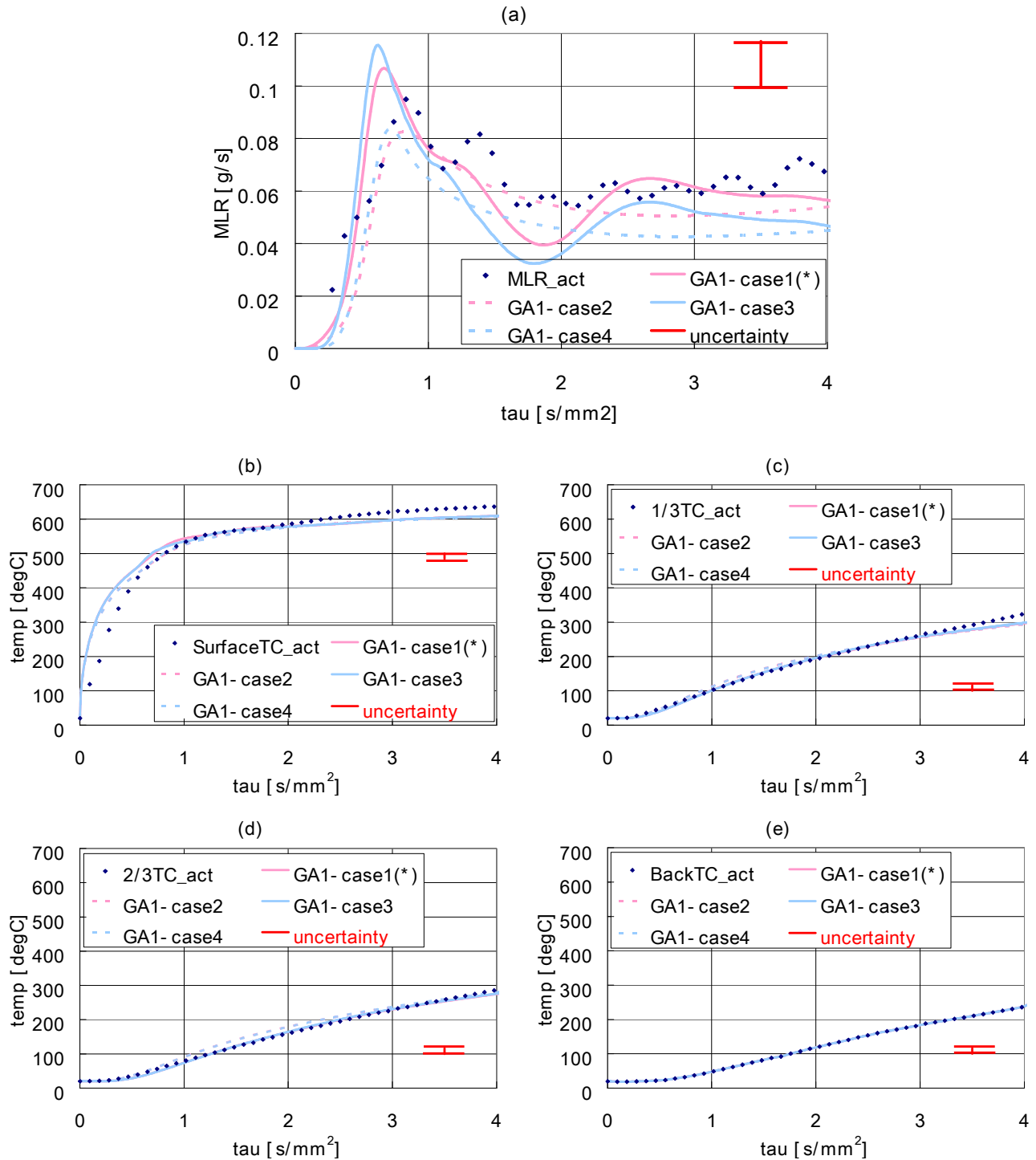


Figure 3: Estimated activation energy of unsaturated brominated polyester resin calculated via “isoconversional” (model free) method



**Figure 4: Kinetic parameters estimated for brominated, unsaturated polyester resin: 3 steps mechanism with nth order kinetic model (a,b) and one step mechanism with nth order kinetic model (c,d)**



**Figure 5. Parameter estimation GA1 results for brominated, unsaturated polyester composite with low glass content (1A) – heterogeneous microstructure and 3 steps degradation mechanism (case1, \* indicates this condition is identical to that of GA1); homogeneous structure and 3 steps degradation mechanism (case2); heterogeneous microstructure and a single step degradation mechanism (case3); homogeneous structure and a single step degradation mechanism (case4) – (a) Mass loss rate; (b) Surface temperature; (c) 1/3 of sample thickness in-depth temperature from the surface; (d) 2/3 of sample thickness in-depth temperature from the surface; (e) Backface temperature**

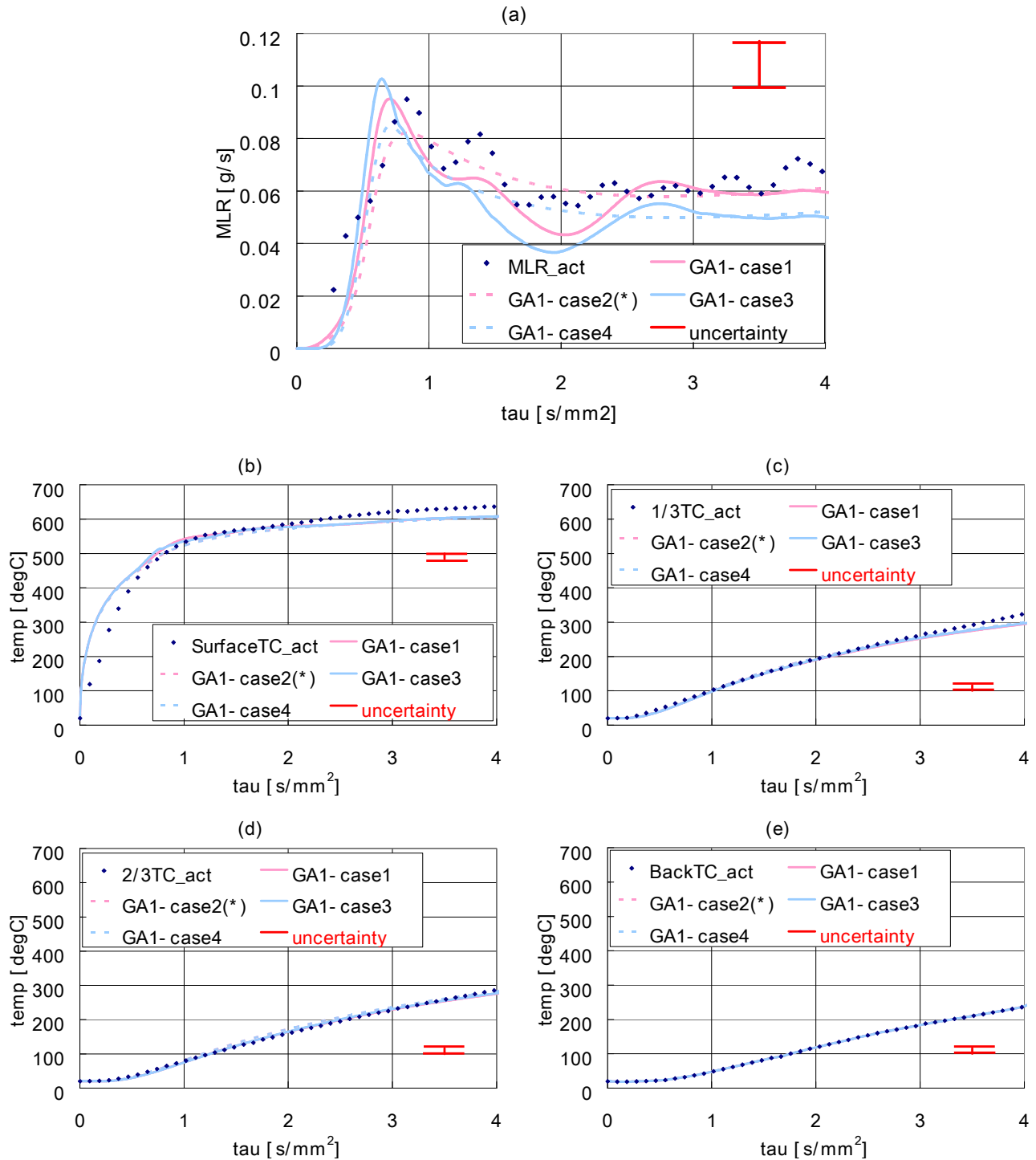


**Figure 6. Parameter estimation GA2 results for brominated, unsaturated polyester composite with low glass content (1A) – heterogeneous microstructure and 3 steps degradation mechanism (case1); homogeneous structure and 3 steps degradation mechanism (case2, \* indicates this condition is identical to that of GA2); heterogeneous microstructure and a single step degradation mechanism (case3); homogeneous structure and a single step degradation mechanism (case4) – (a) Mass loss rate; (b) Surface temperature; (c) 1/3 of sample thickness in-depth temperature from the surface; (d) 2/3 of sample thickness in-depth temperature from the surface; (e) Backface temperature**

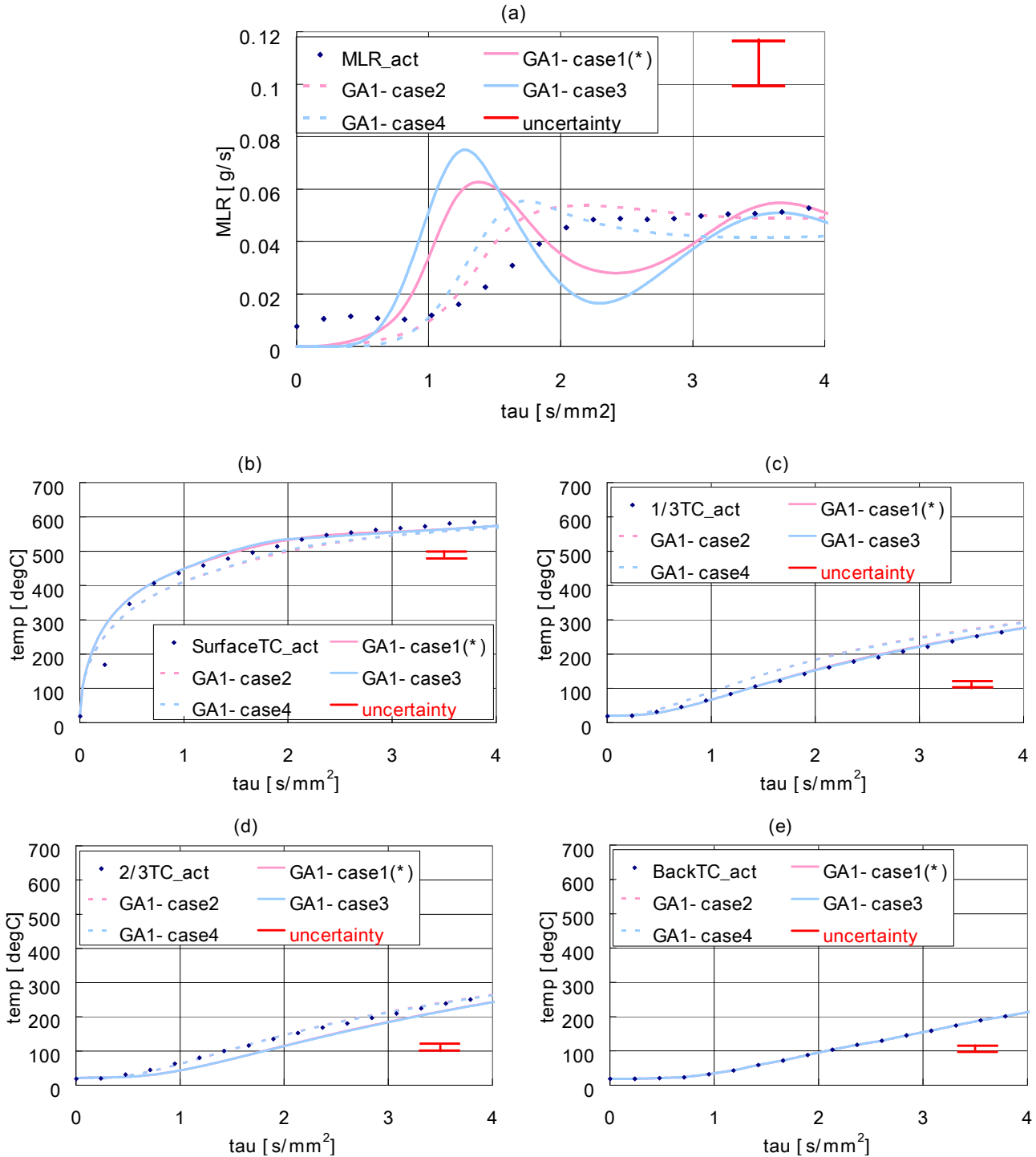


**Figure 7. Pyrolysis modeling results for brominated, unsaturated polyester composite with higher glass content (1C) using estimations based on 1A (GA1) – heterogeneous microstructure and 3 steps degradation mechanism (case1, \* indicates this condition is identical to that of GA1); homogeneous structure and 3 steps degradation mechanism (case2); heterogeneous microstructure and a single step degradation mechanism (case3); homogeneous structure and a single step degradation mechanism (case4) – (a) Mass loss rate; (b) Surface temperature; (c) 1/3 of sample thickness in-depth temperature from the surface; (d) 2/3 of sample thickness in-depth temperature from the surface; (e) Backface temperature**

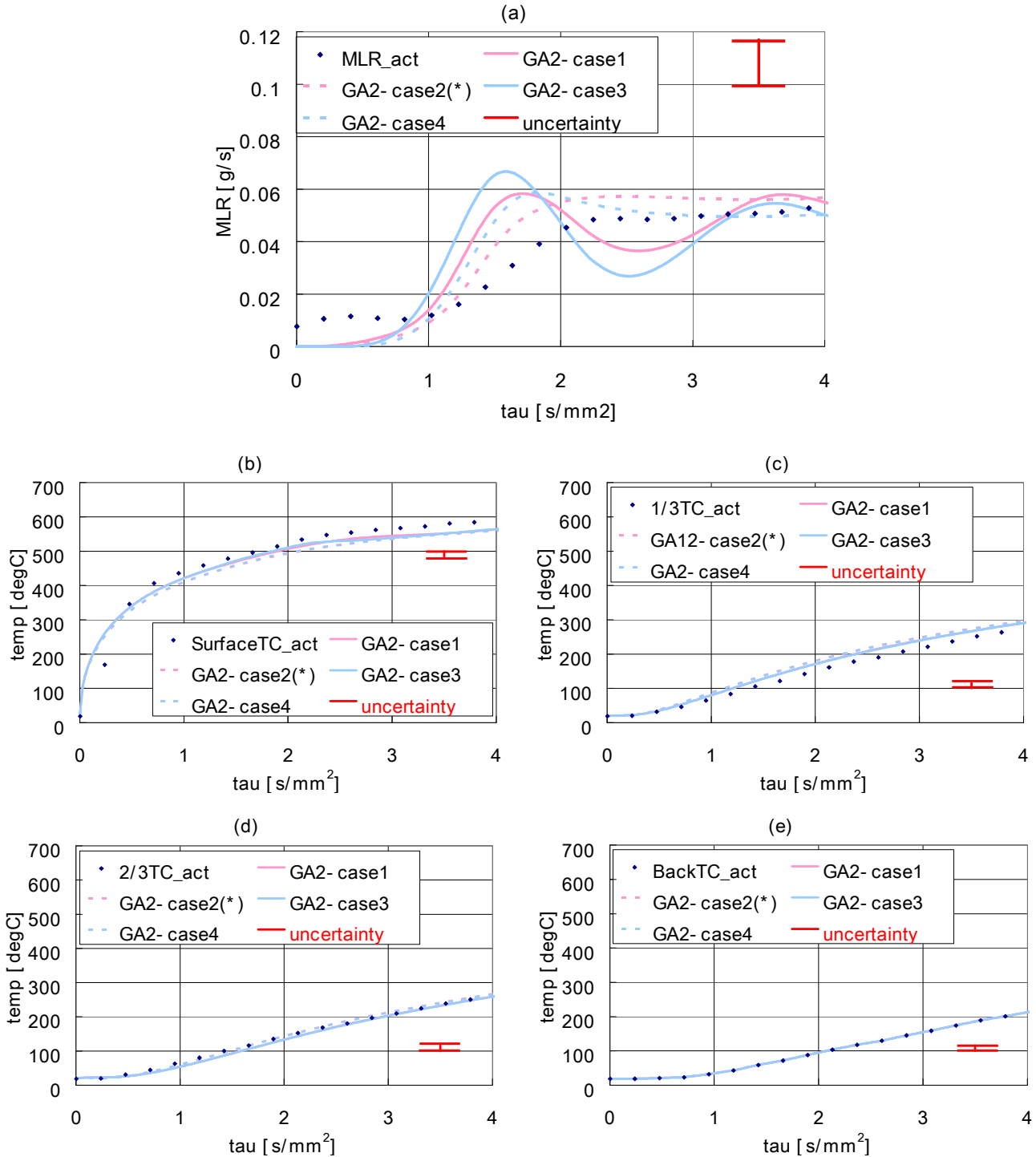


**Figure 8: Pyrolysis modeling results for brominated, unsaturated polyester composite with higher glass content (1C) using estimations based on 1A (GA2) – heterogeneous microstructure and 3 steps degradation mechanism (case1); homogeneous structure and 3 steps degradation mechanism (case2, \* indicates this condition is identical to that of GA2); heterogeneous microstructure and a single step degradation mechanism (case3); homogeneous structure and a single step degradation mechanism (case4) – (a) Mass loss rate; (b) Surface temperature; (c) 1/3 of sample thickness in-depth temperature from the surface; (d) 2/3 of sample thickness in-depth temperature from the surface; (e) Backface temperature**

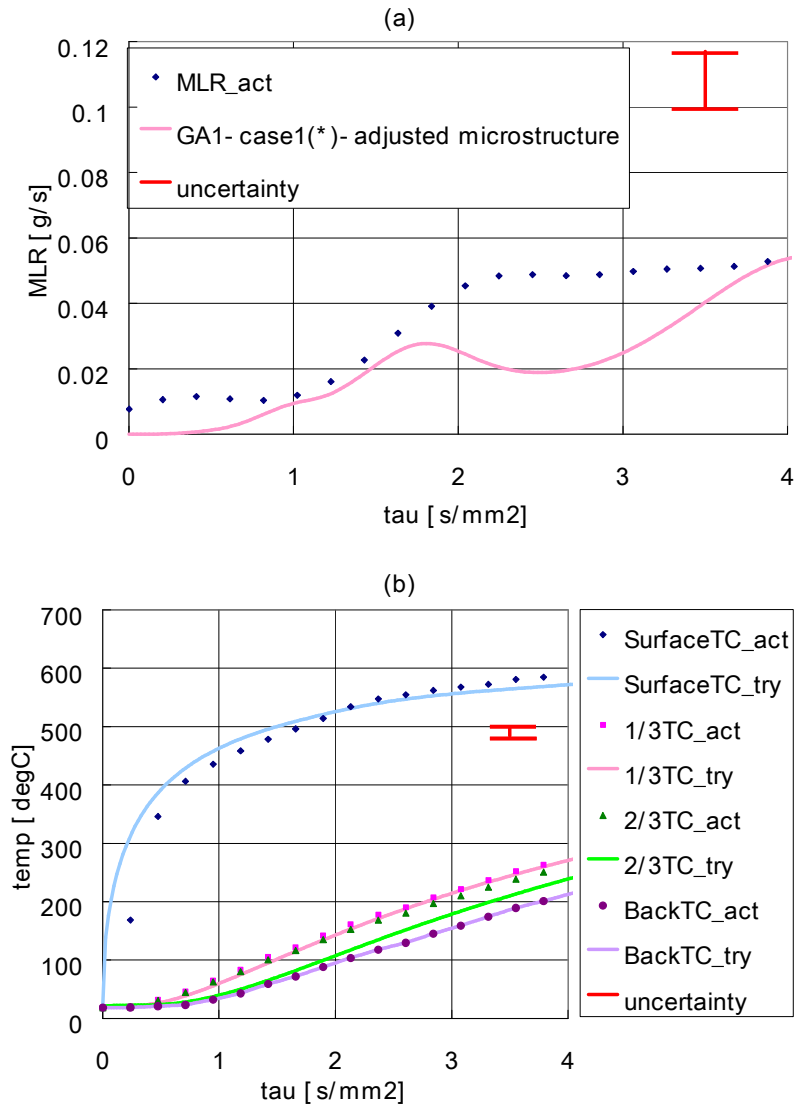


**Figure 9. Pyrolysis modeling results for brominated, unsaturated polyester composite with higher glass content (1C) using estimations based on 1A (GA1) but with 1C microstructure near surface slightly adjusted to account for less resin – heterogeneous microstructure and 3 steps degradation mechanism (case1, \* indicates this condition is identical to that of GA1) – (a) Mass loss rate; (b) Temperature comparisons at various depths (surface, 1/3 and 2/3 of sample thickness in-depth from the surface, and back-face temperatures)**



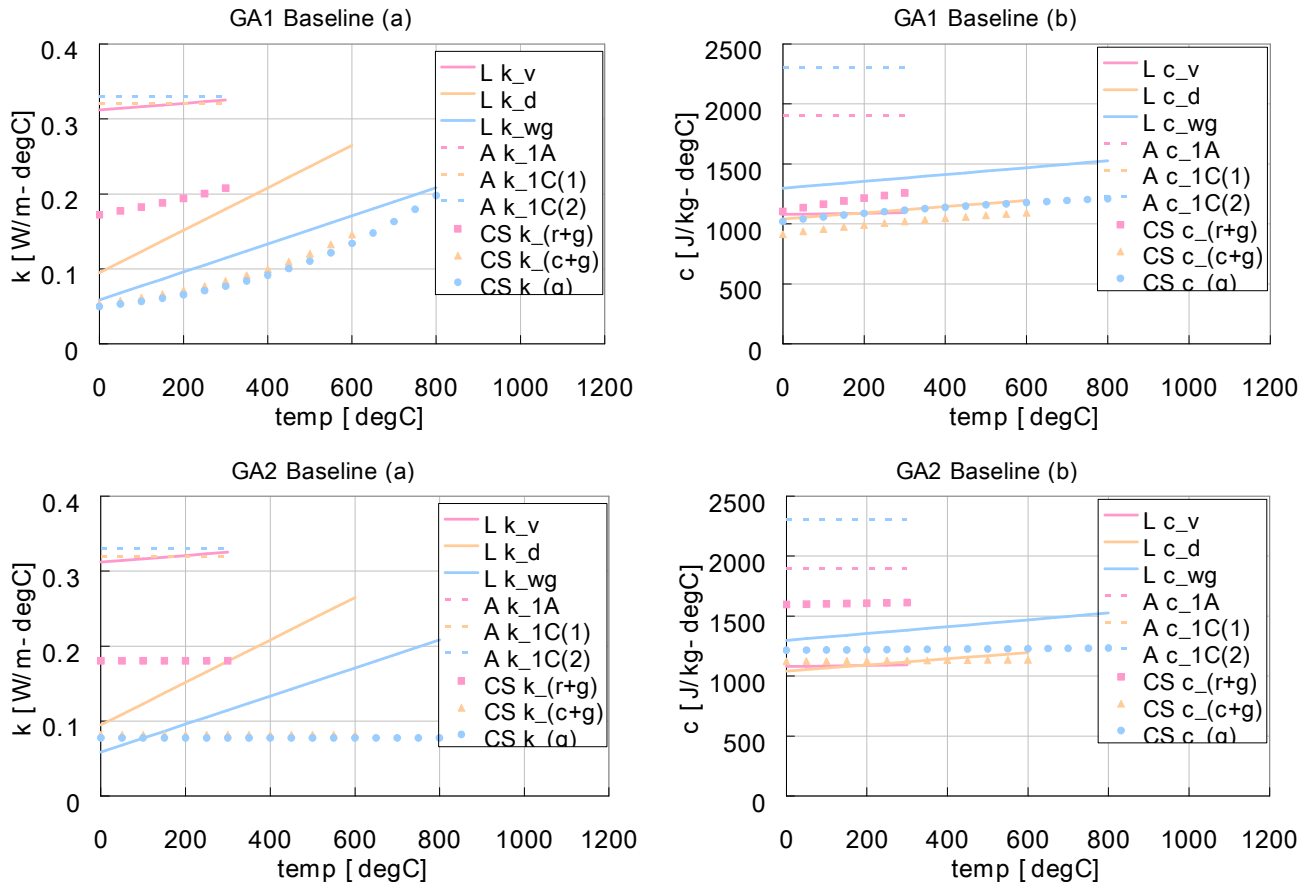


**Figure 10: Estimated parameters with two different baselines – GA1 (heterogeneous structure with three steps of degradation kinetic model) and GA2 (homogeneous structure with three steps of degradation kinetic model) estimations – from current study (CS), conductivity,  $k$  and specific heat capacity,  $c$  for resin and glass (r+g), char and glass (c+g) and glass only (g) assuming constant volume compared with those from the work of Lattimer (L, estimation for virgin composite (v), decomposed composite (d) and woven glass only composite after fully degrading resin (wg)) and Avila (A, estimation for 1A and 1C composites, same samples used in this study).**

**Tables:**

**Table 1: Kinetic parameters estimated from model fitting exercise using Genetic Algorithm (GA): Three steps nth order kinetic model and single step nth order kinetic model**

Kinetics	$Z_1$ (s-1)	$E_{a1}$ (kJ/mol)	$n_1$ (-)	$Z_2$ (s-1)	$E_{a2}$ (kJ/mol)	$n_2$ (-)	$Z_3$ (s-1)	$E_{a3}$ (kJ/mol)	$n_3$ (-)
3 steps nth order	$3.42 \times 10^2$	56.1	1.03	$3.55 \times 10^{11}$	174.1	0.80	$1.75 \times 10^6$	127.6	2.64
Single step nth order				$4.92 \times 10^9$	151.4	0.90			

**Table 2: Optimized thermophysical properties from 1A with heterogeneous assumption. For each material (resin, beta-resin, char, residue and glass) conductivity ( $k_0$ ), conductivity temperature dependency ( $n_k$ ), heat capacity ( $c_0$ ), heat capacity temperature dependency ( $n_c$ ), emissivity ( $\epsilon$ ) and the fitting parameter for radiation heat transfer across pores ( $\gamma$ ) are estimated. Additionally, heat of reaction ( $\Delta H$ ) for three resin decomposition kinetic is estimated.**

Species		$\rho_0$	$k_0$	$n_k$	$c_0$	$n_c$	$\epsilon$	$\gamma$
		(kg/m <sup>3</sup> )	(W/m-K)	(-)	(J/kg-K)	(-)	(-)	(m)
Resin	GA1	1350	0.304	0.082	1185	0.093	0.964	0.0000
	GA2		0.261	0.099	1237	0.206	0.969	0.0000
	GA1-GA2 /GA1 (%)		14.1	19.9	4.4	120.6	0.6	0.0
Beta resin	GA1	1080	0.317	0.080	1260	0.094	0.973	0.0000
	GA2		0.274	0.087	1318	0.207	0.965	0.0000
	GA1-GA2 /GA1 (%)		13.5	9.1	4.6	119.5	0.8	0.0
Char	GA1	95	0.163	0.326	1111	0.464	0.990	0.0046
	GA2		0.169	0.237	1029	0.246	0.991	0.0034
	GA1-GA2 /GA1 (%)		3.4	27.4	7.4	46.9	0.1	0.0
Residue	GA1	41	0.168	0.333	1061	0.481	0.985	0.0046
	GA2		0.176	0.236	956	0.247	0.980	0.0036
	GA1-GA2 /GA1 (%)		4.6	29.1	9.9	48.7	0.4	0.0
Glass	GA1	2600	0.064	0.328	1069	0.249	0.981	0.0034
	GA2		0.113	0.218	1072	0.194	0.982	0.0050
	GA1-GA2 /GA1 (%)		74.9	33.4	0.2	22.3	0.1	0.0
Heat of reaction $\Delta H$ (J/kg)		Degradation Reactions				GA1	GA2	GA1-GA2 /GA1 (%)
		resin $\rightarrow v_{br}$ beta_resin + (1 - $v_{br}$ )gas				3.1E+04	2.2E+04	29.9
		beta_resin $\rightarrow v_c$ char + (1 - $v_c$ )gas				1.1E+05	8.0E+04	29.9
		char $\rightarrow v_r$ residue + (1 - $v_r$ )gas				1.1E+04	8.0E+03	29.9

**Table 3: Testing matrix for parameter estimation of 1A and pyrolysis modeling of 1C – GA1 (case 1: heterogeneous structure and three steps degradation kinetic model) and GA2 (case 2: homogeneous structure and three steps degradation kinetic model) are used to optimize the parameter estimation. Using the estimated values, cases 1 through 4 are simulated using a pyrolysis model [3,4].**

Parameter Estimation	Pyrolysis Modeling	Microstructure	Resin Degradation Kinetics $f(\alpha) = (1 - \alpha)^n$
GA1	Case 1	Heterogeneous	3 steps
	Case 2	Homogeneous	3 steps
	Case 3	Heterogeneous	Single step
	Case 4	Homogeneous	Single step
GA2	Case 1	Heterogeneous	3 steps
	Case 2	Homogeneous	3 steps
	Case 3	Heterogeneous	Single step
	Case 4	Homogeneous	Single step